Redox-photosensitised Reactions. Part 12.[1] Effects of Magnesium(II) Ion on the $[Ru(bpy)_3]^{2+}$-Photomediated Reduction of Olefins by 1-Benzyl-1,4-dihydronicotinamide: Metal-ion Catalysis of Electron Transfer Processes Involving an NADH Model

Osamu Ishitani, Mikio Ihama, Yoji Miyauchi, and Chyongjin Pac*
Department of Chemical Process Engineering, Faculty of Engineering, Osaka University, Suita, Osaka 565, Japan

Magnesium(II) ion catalyses the photosensitised reduction of carbon–carbon double bonds of dimethyl fumarate, derivatives of methyl cinnamate, and some other related olefins by 1-benzyl-1,4-dihydronicotinamide (BNAH), which proceeds *via* sequential two-electron transfer initiated by the photoexcitation of $[Ru(bpy)_3]^{2+}$ (bpy = 2,2′-bipyridine). The metal ion forms a complex with BNAH in methanol as well as in 10:1 (v/v) pyridine–methanol, leading to the retardation of electron transfer from BNAH to luminescent excited-state $Ru(ppy)_3^{2+}$. The net metal-ion effects arise from the catalysis of both the first and second one-electron reduction processes.

It is known that Mg^{II} and Zn^{II} ions can catalyse net hydride transfer from the NADH models 1,4-dihydropyridines to unsaturated substrates such as carbonyl and olefinic compounds;[2–5] this constitutes a metal-ion catalysis of biological interest related to the essential role of Zn^{II} ion in enzymatic redox reactions involving the pyridine nucleotide coenzymes.[6] However, it still remains controversial whether the metal ions activate the NADH models,[3,7,8] the substrates,[2,5,9] or both.[10,11] In particular, crucial questions arise as to the mechanistic origin of the catalysis, since the mechanisms of the net hydride transfer continue to be debated, involving the one-step transfer of a hydride ion,[5,12–14] the sequential transfer of an electron and a hydrogen atom,[5,14] or the sequential electron-proton-electron transfer.[11]

In a previous communication,[15] we briefly reported that Mg^{II} enhances the redox-photosensitised reduction of dimethyl fumarate by 1-benzyl-1,4-dihydronicotinamide (BNAH) using $[Ru(bpy)_3]^{2+}$ (bpy = 2,2′-bipyridine) as a photosensitiser. The mechanism of the redox-photosensitised reactions of BNAH with olefinic and carbonyl compounds involves $[Ru(bpy)_3]^{2+}$-photomediated electron transfer from BNAH to substrates followed by electron-transfer and/or radical-coupling reactions between radical intermediates as is shown in Scheme 1.[1,14,15]

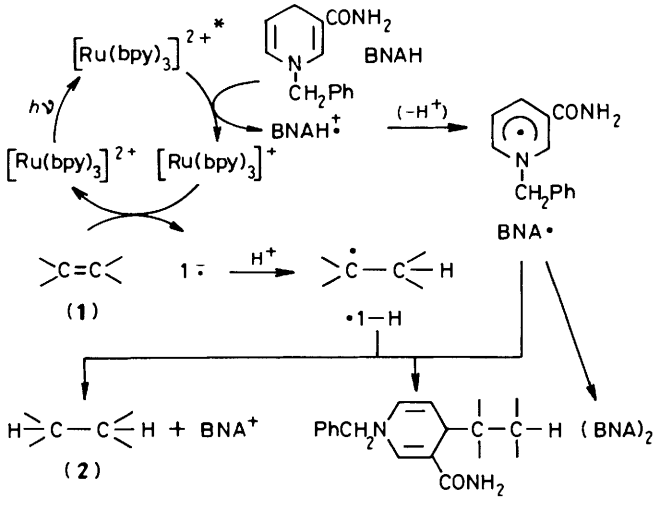

Scheme 1.

Therefore, the effect of Mg^{II} ion on the redox-photosensitised reduction may provide a clue to the catalytic behaviour of the metal ion in electron-transfer reactions of NADH models. We have thus investigated, in some detail, the effect of Mg^{II} ion on the $[Ru(bpy)_3]^{2+}$-photosensitised reduction of dimethyl fumarate and several selected olefins by BNAH.

Results

Net Effect of Mg^{II} *Ion on Photosensitised Reactions.*—The photosensitised reactions were carried out by visible-light (>470 nm) irradiation of methanolic and pyridine–methanol (10:1 v/v) solutions. In the present investigation, $Mg(ClO_4)_2$ was used as the source of Mg^{II} ion at 0.05 or 0.1 mol dm^{-3} in 10:1 pyridine–methanol and at 0.025 mol dm^{-3} in methanol. Higher concentrations of $Mg(ClO_4)_2$ in methanol were avoided because of the precipitation of a red-orange solid upon admixture of the reactants. Scheme 2 shows the products isolated, details of which have been already described

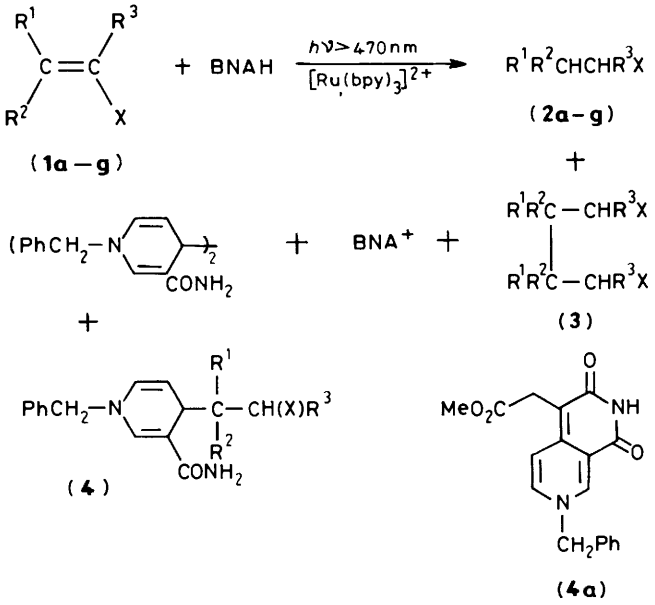

Scheme 2.

Table 1. $[Ru(bpy)_3]^{2+}$-Photosensitised reduction of (**1a**—**g**) by BNAH and effects of Mg^{II} ion[a]

	Olefin				Irrad.		Convn. of (1) (%)[c]		Yield of (2) (%)[c,d]	
	R^1	R^2	R^3	X	Time (m)	Solvent[b]	Without Mg^{2+}	With Mg^{2+}	Without Mg^{2+}	With Mg^{2+}
(**1a**)	CO_2Me	H	H	CO_2Me	20	A	67	72	40	80
						B	58	93	70	80
(**1b**)	*p*-C_6H_4CN	H	H	CO_2Me	20	A	49	49	63	83
						B	74	96	100	100
(**1c**)	*p*-$C_6H_4CO_2Me$	H	H	CO_2Me	20	A	17	22	70	90
						B	58	86	72	90
(**1d**)	Ph	Ph	H	CO_2Me	100	A	22	42	59	88
						B	15	31	25	57
(**1e**)	H	Ph	Ph	CN	60	B	22	67	30	47
(**1f**)	Ph	Ph	H	CN	60	B	38	60	32	55
(**1g**)	Ph	H	Ph	COMe	20	B	24	87	0	7

[a] For 3-cm^3 solutions irradiated at >470 nm. [b] A = methanolic solutions containing $[Ru(bpy)_3]^{2+}$ (0.3 mmol dm^{-3}), BNAH (25 mmol dm^{-3}), (**1a**—**g**) (12.5 mmol dm^{-3}), and $Mg(ClO_4)_2$ (25 mmol dm^{-3}); B = 10:1 pyridine–methanol solutions containing $[Ru(bpy)_3]^{2+}$ (1.0 mmol dm^{-3}), BNAH (100 mmol dm^{-3}), (**1a**—**g**) (50 mmol dm^{-3}), and $Mg(ClO_4)_2$ (50 mmol dm^{-3}). [c] Conversion and yields at level-off points determined by v.p.c. [d] Based on (**1a**—**g**) unrecovered.

Table 2. Relative quantum yields in the presence and absence of Mg^{II} ion[a,b]

Olefin	$-E_{1/2}^{red}$(V)[c]	$-E_{1/2}^{pre}$(V)[d]	ΔE(V)[e]	Solvent	$\varphi_{-1}^{M}/\varphi_{-1}$	φ_2^{M}/φ_2	φ_2/φ_{-1}	$(\varphi_2/\varphi_{-1})^{M}$
(**1a**)	1.72	1.49	0.23	A	1.1	2.0	0.41	0.80
				B	1.6	1.6	0.85	0.86
(**1b**)	1.80	1.63	0.17	A	1.0	1.3	0.72	0.92
				B	1.3	1.3	1.0	1.0
(**1c**)	1.88	1.65	0.23	A	1.1	1.4	0.7	0.85
				B	1.7	1.7	1.0	1.0
(**1e**)	1.95	1.82	0.13	B	2.1	3.6	0.37	0.63

[a] Relative quantum yields determined at the concentrations of the reactants described in the footnote of Table 1. [b] The quantum-yield abbreviations with and without superior M denote those with and without Mg^{II} ion. [c] Polarographic reduction potentials *vs.* Ag/$AgNO_3$ in MeCN. [d] Half-wave potentials of pre-waves observed with $Mg(ClO_4)_2$ one-half equivalent to the olefins. [e] $E_{1/2}^{pre} - E_{1/2}^{red}$.

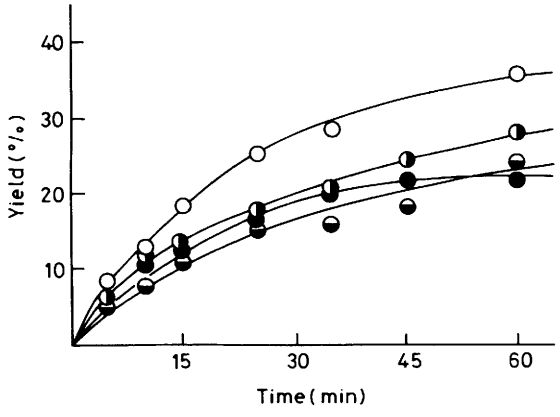

Figure 1. Effects of added salts on the formation of (**2c**) by the $[Ru(bpy)_3]^{2+}$-photosensitised reduction of (**1c**) by BNAH in MeOH; no added salt (●), $LiClO_4$ (50 mmol dm^{-3}) (◑), NH_4ClO_4 (50 mmol dm^{-3} (◒), $Mg(ClO_4)_2$ (25 mmol dm^{-3}) (○); $[Ru(bpy)_3^{2+}]$ 0.3 mmol dm^{-3}, [BNAH] 25 mmol dm^{-3}, [(**1a**)] 12.5 mmol dm^{-3}; irradiation at >470 nm

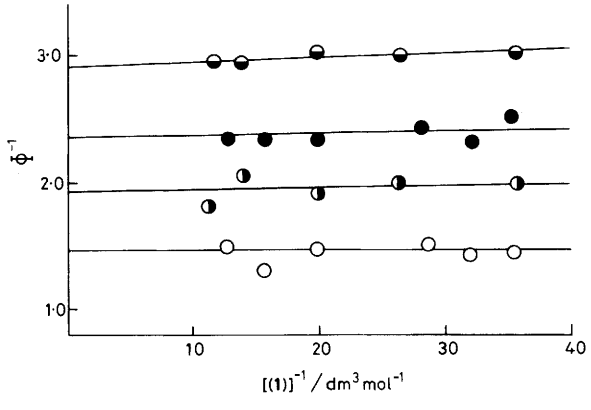

Figure 2. Double-reciprocal plots of quantum yield *vs.* concentration of (**1a**) for the disappearance of (**1a**) with (○) and without (●) Mg^{2+} and for the formation of (**2a**) with (◑) and without (◒) Mg^{2+}; $[Ru(bpy)_3^{2+}]$ 1.0 mmol dm^{-3}, [BNAH] 0.1 mol dm^{-3}, $[Mg^{2+}]$ 0.1 mol dm^{-3} in 10:1 pyridine–methanol; irradiation at 520 nm

elsewhere.[1] In the present investigation, both the disappearance of (**1a**—**g**) and the formation of (**2a**—**g**) were followed by v.p.c., while the other products were not analysed. It was confirmed that no reaction occurs in the dark. Moreover, (**3**) and (**4**) gave neither (**1**) nor (**2**) under the photoreaction conditions with $Mg(ClO_4)_2$.

Table 1 summarises conversions of (**1a**—**g**) and chemical yields of (**2a**—**g**) in the presence or absence of $Mg(ClO_4)_2$ and Table 2 lists relative quantum yields for the disappearance of (**1**) (φ_{-1} and φ_{-1}^{M}) and the formation of (**2**) (φ_2 and φ_2^{M}) together with half-wave reduction potentials of (**1**) ($E_{1/2}^{red}$), and other electrochemical data (*vide infra*). These results clearly demonstrate the catalytic effects of $Mg(ClO_4)_2$, which are specific for Mg^{II} ion since neither NH_4ClO_4 nor $LiClO_4$ exerts much effect

Table 3. Equilibrium constants for equation (1) and luminescence-quenching rate constants

Solvent[a]	K (dm^3 mol^{-1})	τ^b (ns)	k_q^{app} (dm^3 mol^{-1} s^{-1})	k_q^B (dm^3 mol^{-1} s^{-1})	k_q^C (dm^3 mol^{-1} s^{-1})
A	7	730 (800)	1.4×10^8	1.5×10^8	9×10^7
B	42	850 (960)	1.1×10^8	3.7×10^8	*ca.* 5×10^6

[a] A = methanol and B = 10:1 (v/v) pyridine–methanol. [b] The observed luminescence lifetimes of $[Ru(bpy)_3]^{2+}$ at 20 °C in the presence of $Mg(ClO_4)_2$ at 25 mmol dm^{-3} in MeOH and at 0.1 mol dm^{-3} in pyridine–methanol. In parentheses are the lifetimes without Mg^{2+}.

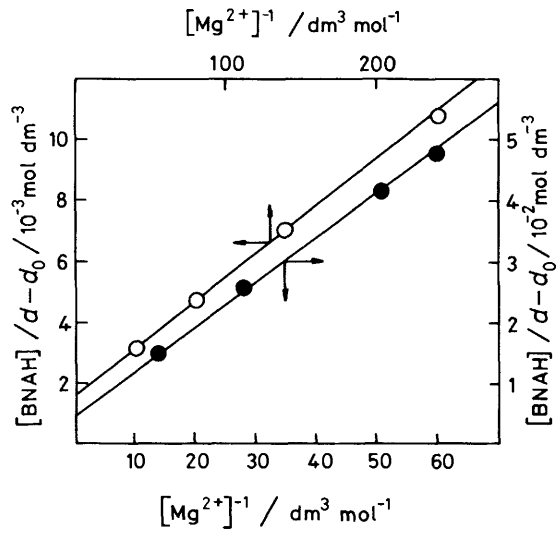

Figure 3. Ketelaar's plots for the complex formation of BNAH with Mg^{2+} in MeOH (●) and in 10:1 pyridine–methanol (○); [BNAH] 1.0 mmol dm^{-3}

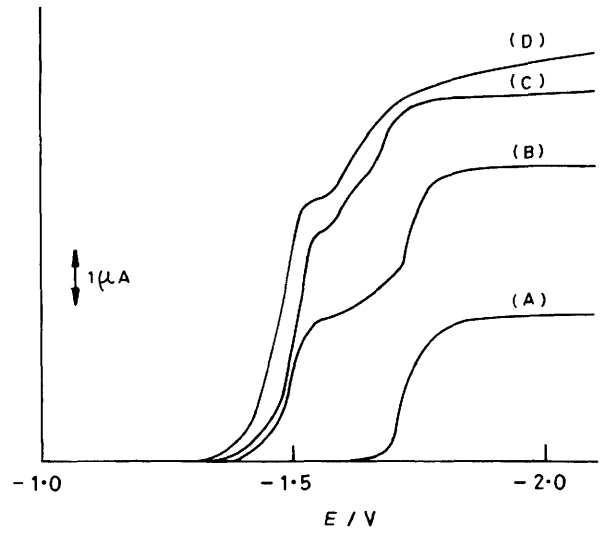

Figure 4. Polarograms of (**1a**) without Mg^{2+} (A) and with $Mg(ClO_4)_2$ at 0.45 (B), 1.0 (C), and 2.0 mmol dm^{-3} (D) in deaerated MeCN; [(**1a**)] 1.0 mmol dm^{-3}, [Et_4NClO_4] 0.1 mol dm^{-3}; scan rate 5 mV s^{-1}

on the photosensitised reduction of (**1c**) as is shown in Figure 1. It was found that the quantum yields for the photoreduction of (**1a**) are almost independent of concentration of (**1a**) (Figure 2).

Interactions of Mg^{II} *Ion with* BNAH *and Olefins.*—It is known that NADH models form complexes with Mg^{II} and Zn^{II} ions.[3,16,17] Although Mg^{II} ion caused only a little shift of the absorption maximum of BNAH at $<10^{-4}$ mol dm^{-3} in either methanol or pyridine–methanol (10:1), the end absorption of BNAH at a relatively high concentration (1×10^{-3} mol dm^{-3}) significantly increases with concentration of $Mg(ClO_4)_2$. The spectral change was analysed according to the Ketelaar's equation[18] [equation (1)], where d and d_0 represent optical

$$\text{BNAH} + Mg^{2+} \underset{}{\overset{K}{\rightleftharpoons}} \text{BNAH-}Mg^{2+} \equiv C \qquad (1)$$

$$\frac{[\text{BNAH}]}{d - d_0} = \frac{1}{\varepsilon_c - \varepsilon_b}\left(1 + \frac{1}{K[Mg^{2+}]}\right) \qquad (2)$$

densities at 410 nm in the presence and absence of $Mg(ClO_4)_2$, respectively; ε_b and ε_c denote the molar absorption coefficients at 410 nm for free BNAH and the BNAH-Mg^{2+} complex, respectively. Figure 3 shows double-reciprocal plots of $(d - d_0)$ *vs.* $[Mg^{2+}]$, the intercepts and slopes of which give the equilibrium constants, K. The observed values listed in Table 3 are smaller by two or three orders of magnitude than those reported for pairs of the same or similar NADH models and Mg^{2+} or Zn^{2+};[3,6,16,17] the metal ion is stabilised by the co-ordination of methanol.

On the other hand, no complex formation between Mg^{II} ion and the olefins was indicated by spectroscopic measurements; admixture of $Mg(ClO_4)_2$ in an equimolar caused no essential change in i.r. spectra of KBr discs, $CHCl_3$ solutions, and Nujol mulls, u.v. spectra of methanolic solutions, and ^1H and ^{13}C n.m.r. spectra of CD_3CN solutions.

In contrast, Mg^{II} ion remarkably affected polarographic behaviours of the olefins such that pre-waves appear at more positive potentials than $E_{1/2}^{red}$ and increase in currents with an increase in concentration of Mg^{II} ion (Figure 4). Table 2 includes the half-wave potentials of the pre-waves ($E_{1/2}^{pre}$), which were taken with $Mg(ClO_4)_2$ in an amount of one-half equiv. to each olefin, where the pre-waves clearly appeared without significant effects of adsorption on the electrode. Since Mg^{2+} does not form complexes with the olefins as discussed above, the appearance of the pre-waves is not static but dynamic in nature, probably arising from the stabilisation of the anion radical of the olefins by ion pairing or complex formation with Mg^{2+} on the electrode.[19]

$$(1) + e^- \rightleftharpoons (1)^{-\cdot} \overset{Mg^{2+}}{\rightleftharpoons} Mg^{2+} \cdots (1)^{-\cdot}$$

Discussion

The luminescence of $[Ru(bpy)_3]^{2+}$ was quenched by BNAH either without or with Mg^{II} ion following linear Stern-Volmer relationships. The Stern-Volmer constants when Mg^{II} ion is present are smaller than those in its absence. Since the luminescence lifetimes are little affected by Mg^{II} ion, the

apparent quenching rate constants (k_q^{app}) are the quantities to be examined for the metal-ion effects. If the luminescence quenching occurs with both free BNAH and the BNAH-Mg^{2+} complex with rate constants of k_q^B and k_q^C respectively, equation (3) gives an approximate kinetic representation of

$$\frac{\varphi_L}{\varphi_L^Q} = 1 + k_q^{app}\tau c_B \simeq 1 + \left[k_q^B - (k_q^B - k_q^C)\left(\frac{K \cdot c_M}{1 + K \cdot c_M}\right)\right]\tau c_B \quad (3)$$

k_q^{app} in cases where $c_B \ll c_M$; c_B and c_M denote the total concentrations of BNAH and $Mg(ClO_4)_2$ respectively. Table 3 lists the calculated values of k_q^C together with k_q^B and K. Since $k_q^B > k_q^C$ in each case, the complex formation evidently suppresses the electron-donating capabilities of BNAH, an observation in line with Mg^{2+}-induced positive shifts of the electrochemical oxidation wave of BNAH.[20]

It should be noted however that complex formation has little effect on the photoreduction, since $k_q^B(c_B - [C]) \gg k_q^C[C]$ under the photoreaction conditions. In other words, only free BNAH participates in the initiation process of the photosensitised reactions even in the presence of Mg^{II} ion, *i.e.*, electron transfer from free BNAH to luminescent excited-state $[Ru(bpy)_3]^{2+}$ (^{3}MLCT) [equation (5)].[1,15] This means that the observed effects of Mg^{II} ion are not static but dynamic in nature. Calculations show that net quenching of ^{3}MLCT by BNAH with or without Mg^{II} ion under the photoreaction conditions is complete in pyridine–methanol (10:1) and similar in efficiency (72% and 75%, respectively) in methanol.

The quantum yields for the disappearance of (**1**) are diagnostic for possible effects of Mg^{II} ion on the processes involved in the first one-electron reduction of (**1**), [equations (4)—(9)]; the probabilities of equations (5a) and (8) occurring

$$[Ru(bpy)_3]^{2+} \xrightarrow{h\nu} {}^3\text{MLCT} \quad (4)$$

$$^3\text{MLCT} + \text{BNAH} \xrightarrow{k_q^B} \{[Ru(bpy)_3]^+ \; BNAH^{+\bullet}\} \xrightarrow{P_1(P_1^M)} [Ru(bpy)_3]^+ + BNAH^{+\bullet} \quad (5a)$$

$$\{[Ru(bpy)_3]^+ \; BNAH^{+\bullet}\} \xrightarrow{1-P_1(P_1^M)} [Ru(bpy)_3]^{2+} + \text{BNAH} \quad (5b)$$

$$[Ru(bpy)_3]^+ + (\mathbf{1}) \xrightarrow{k_6} [Ru(bpy)_3]^{2+} + (\mathbf{1})^{-\bullet} \quad (6)$$

$$[Ru(bpy)_3]^+ + X \xrightarrow{k_7} [Ru(bpy)_3]^{2+} + X_{red} \quad (7)$$

$$(\mathbf{1})^{-\bullet} + H^+(\text{Solvent} \xrightarrow{P_2(P_2^M)} {}^\bullet(\mathbf{1})\text{-H} \quad (8)$$

$$(\mathbf{1})^{-\bullet} + Y \xrightarrow{1-P_2(P_2^M)} (\mathbf{1}) + Y_{red} \quad (9)$$

(X and Y; impurities)

are represented by P_1 and P_2 without Mg^{2+} or by P_1^M and P_2^M with the metal ion, respectively. The regeneration of (**1**) from $^\bullet$(**1**)-H can be neglected since the photoreduction of (**1a**) and dimethyl maleate in MeOD results in no deuterium incorporation in the recovered olefins as well as in no stereomutation.[15] In the case of (**1a**), moreover, both the quantum yields for the disappearance of (**1a**) and for the formation of (**2a**) are independent of the concentration of (**1a**) in either the presence or absence of Mg^{II} ion, thus demonstrating that $k_6[(\mathbf{1a})]/k_7$ is unaffected by Mg^{II} ion. Therefore, equation (10) represents the metal-ion effects on the first one-electron reduction of (**1a**) and may also hold in cases of the other olefins.

$$\frac{\varphi_{-1}^M}{\varphi_{-1}} = \left(\frac{P_1^M}{P_1}\right) \times \left(\frac{P_2^M}{P_2}\right) \quad (10)$$

Since $\varphi_{-1}^M > \varphi_{-1}$ in pyridine–methanol (10:1), Mg^{II} ion may enhance the separation of the ion pair, $\{[Ru(bpy)_3]^+ \; BNAH^{+\bullet}\}$, by microenvironmental electrostatic effects and/or may stabilise $(\mathbf{1})^{-\bullet}$ by ion pairing or complex formation to prevent the loss of an electron from $(\mathbf{1})^{-\bullet}$ as is shown in equation (11). Although P_1 (P_1^M) and P_2 (P_2^M) cannot be

$$(\mathbf{1})^{-\bullet} + Mg^{2+} \rightleftharpoons Mg^{2+} \cdots (\mathbf{1})^{-\bullet} \xrightarrow[(-Mg^{2+})]{H^+} {}^\bullet(\mathbf{1})\text{-H} \quad (11)$$

factored out from φ_{-1} (φ_{-1}^M) by usual steady-state kinetics, the appearance of the pre-waves in the electrochemical reduction of (**1**) in the presence of Mg^{II} ion suggests that equation (11) is an important pathway for the metal-ion effects in 10:1 pyridine–methanol. On the other hand, Mg^{II} ion had little effect on the disappearance of (**1**) in methanol this being particularly so for (**1a**), (**1b**), and (**1c**). In this solvent, $(\mathbf{1})^{-\bullet}$ may be much more efficiently protonated than the loss of an electron and/or the Mg^{II} ion exclusively exists as $[Mg(MeOH)_6]^{2+}$ that may be inactive in the stabilisation of $(\mathbf{1})^{-\bullet}$.

The formation of (**2**) after the one-electron reduction involves the deprotonation of $BNAH^{+\bullet}$ [equation (12a)], and the one-electron reduction of $^\bullet$(**1**)-H by BNA$^\bullet$ [equation (13a)], as key mechanistic pathways. The net efficiency for the formation of (**2**) from $^\bullet$(**1**)-H can be represented by φ_2/φ_{-1} without Mg^{II} ion or by $(\varphi_2/\varphi_{-1})^M$ with the metal ion, which approximately equals $P_3 \cdot P_4$ or $P_3^M \cdot P_4^M$ each; P_3 (P_3^M) and P_4 (P_4^M) denote the efficiencies of equations (12a) and (13a), respectively, in the absence (presence) of Mg^{II} ion.

$$BNAH^{+\bullet} \xrightarrow[\text{Base}]{P_3(P_3^M)} BNA^\bullet + H^+(\text{Base}) \quad (12a)$$

$$BNAH^{+\bullet} \xrightarrow{1-P_3(P_3^M)} \text{Others} \quad (12b)$$

$$^\bullet(\mathbf{1})\text{-H} + BNA^\bullet \xrightarrow{P_4(P_4^M)} (\mathbf{2}) + BNA^+ \quad (13a)$$

$$^\bullet(\mathbf{1})\text{-H} + BNA^\bullet \xrightarrow{1-P_4(P_4^M)} \text{Others} \quad (13b)$$

Since the rapid abstraction of a proton from $BNAH^{+\bullet}$ by pryidine has been well established,[21] it is reasonable to assume that $P_3 \approx P_3^M \approx 1$ in 10:1 pyridine–methanol and hence that $\varphi_2/\varphi_{-1} \approx P_4$ and $(\varphi_2/\varphi_{-1})^M \approx P_4^M$ in this solvent. In other words, the quantum-yield ratios in 10:1 pyridine–methanol or, less accurately, the yields of (**2**) in Table 1 provide a convenient clue to the effects of Mg^{II} ion on equation (13a). However, it should be noted that such presumptions are valid only in cases where $\varphi_2/\varphi_{-1} < 1$. For (**1a**), (**1b**), (**1c**), no metal-ion effect was observed since $\varphi_2/\varphi_{-1} \approx 1$.

In the case of (**1e**), $(\varphi_2/\varphi_{-1})^M$ is significantly greater than φ_2/φ_{-1}, and the yield of (**2d**) with Mg^{II} ion is twice as high as that without the metal ion. In sharp contrast to the complete lack of the photoreduction to (**2g**) without the metal ion, the photosensitised reduction of (**1g**) to (**2g**) did occur in the presence of Mg^{II} ion in low yield. These observations clearly demonstrate that Mg^{II} ion catalyses the electron transfer from BNA$^\bullet$ to $^\bullet$(**1**)-H. The mechanism of the catalysis is, perhaps, similar to that discussed in the metal-ion effect on the first one-electron reduction of (**1**) as follows.

$$BNA^\bullet + {}^\bullet(\mathbf{1})\text{-H} \rightleftharpoons BNA^+ + {}^-(\mathbf{1})\text{-H} \xrightarrow{Mg^{2+}} Mg^{2+} \cdots {}^-(\mathbf{1})\text{-H}$$

It was found that $(\varphi_2/\varphi_{-1})^M > \varphi_2/\varphi_{-1}$ in the photoreduction of (**1a**), (**1b**), and (**1c**) in MeOH. In this solvent, however, possible effects on equation (12a) should be taken into account, since $P_3 < 1$ because of the low basic nature of MeOH.[21] The deprotonation of $BNAH^{+\bullet}$ would be enhanced by the additional positive charge upon encounter with Mg^{II} ion.

Experimental

Methanol was distilled from magnesium methoxide. Pyridine was refluxed over anhydrous KOH and then distilled before use. BNAH[22] and $[Ru(bpy)_3]Cl_2 \cdot 6H_2O$[23] were prepared according to the literature methods. Dimethyl fumarate, (**1a**), was reagent grade (Tokyo Kasei). The other olefins were prepared according to methods described elsewhere.[1] $Mg(ClO_4)_2$, $LiClO_4$, and NH_4ClO_4 were thoroughly dried by heating at 120 °C *in vacuo* for > 20 h.

Analytical v.p.c. was carried out on a Shimadzu GC-3BF machine with flame ionisation detectors using a 2 m × 4 mm column packed with 2% OV-17 on Shimalite W. ^1H N.m.r. spectra were recorded on a JEOL JNM-PS-100 spectrometer, ^{13}C n.m.r. spectra on a JEOL JNM-FX-100 spectrometer, i.r. spectra on a Hitachi 260-10 spectrometer, u.v. and visible absorption spectra on a Hitachi 220-A spectrometer, and emission spectra on a Hitachi MPF-4 spectrofluorometer.

Polarographic measurements were carried out for N_2-saturated dry acetonitrile solutions at 20 ± 0.1 °C using a dropping mercury electrode, an $Ag/AgNO_3$ (0.1 mol dm^{-3}) reference electrode, Et_4NClO_4 (0.1 mol dm^{-3}) as the supporting electrolyte, and a Yanagimoto P-1000 potentiostat.

Photoreactions and Quantum Yields.—All volumetric flasks, pipettes, and reaction vessels were dried, *in vacuo*, in a desiccator. The concentrations of the sensitiser, BNAH, the olefins, and the salts are indicated in the footnotes of Tables 1 and 2 and Figures 1 and 2. The equipment for irradiation and the filter solution was the same as that reported earlier.[1] Aliquots (3 cm^3) of solutions were introduced into Pyrex tubes (8 mm *i.d.*), deaerated by bubbling with a gentle stream of Ar, and then irradiated with a Matsushita tungsten–halogen lamp (300 W) at > 470 nm under cooling with water using a 'merry-go-round' turntable. Both the disappearance of (**1**) and the formation of (**2**) were followed by v.p.c. and plotted against time (see Figure 1). The conversions of (**1**) and the yields of (**2**) in Table 1 were those at level-off points of the plots. The relative quantum yields in Table 2 were obtained from the slopes of initial linear portion of the plots. The quantum yields in Figure 2 were determined at 520 nm by using a Reinecke's salt actinometer,[24] a Hitachi MPF-2A monochromator, and a xenon lamp. All the procedures were performed in a dark room with a safety lamp.

References

1 Part 11, C. Pac, Y. Miyauchi, O. Ishitani, M. Ihama, M. Yasuda, and H. Sakurai, *J. Org. Chem.*, 1984, **49**, 26.
2 D. J. Creighton and D. S. Sigman, *J. Am. Chem. Soc.*, 1971, **93**, 6314.
3 A. Ohno, H. Yamamoto, T. Okamoto, S. Oka, and Y. Ohnishi, *Bull. Chem. Soc. Jpn.*, 1977, **50**, 2385.
4 Y. Ohnishi, M. Kagami, T. Numakunai, and A. Ohno, *Chem. Lett.*, 1976, 915.
5 R. A. Gase and U. K. Pandit, *J. Am. Chem. Soc.*, 1979, **101**, 7059.
6 S. E. Pattinson and M. F. Dunn, *Biochemistry*, 1976, **15**, 3691 and 3696.
7 A. Ohno, T. Kimura, H. Yamamoto, S. G. Kim, S. Oka, and Y. Ohnishi, *Bull. Chem. Soc. Jpn.*, 1977, **50**, 1535; A. Ohno, S. Yasui, H. Yamamoto, S. Oka, and Y. Ohnishi, *ibid.*, 1978, **51**, 294.
8 M. Hughes and R. H. Prince, *J. Inorg. Nucl. Chem.*, 1978, **40**, 703.
9 R. A. Gase, G. Boxhoorn, and U. K. Pandit, *Tetrahedron Lett.*, 1976, 2889.
10 M. Hughes and R. H. Prince, *Chem. Ind. (London)*, 1975, 648; A. Kitani and K. Sasaki, *J. Electroanal. Chem.*, 1978, **94**, 201.
11 A. Ohno, J. Nakai, K. Nakamura, T. Goto, and S. Oka, *Bull. Chem. Soc. Jpn.*, 1981, **54**, 3482 and references cited therein.
12 B. E. Norcoss, D. E. Klinedinst, and F. J. Westheimer, *J. Am. Chem. Soc.*, 1962, **84**, 797; K. Wallenfels, W. Ertel, and K. Friedlich, *Liebigs Ann. Chem.*, 1973, 1663; I. MacInnes, D. C. Nonhebel, S. T. Orszulik, and C. J. Suckling, *J. Chem. Soc., Perkin Trans. 1*, 1983, 2777.
13 M. F. Powell and T. C. Bruice, *J. Am. Chem. Soc.*, 1983, **105**, 1014.
14 O. Ishitani, C. Pac, and H. Sakurai, *J. Org. Chem.*, 1983, **48**, 2941.
15 C. Pac, M. Ihama, M. Yasuda, Y. Miyauchi, and H. Sakurai, *J. Am. Chem. Soc.*, 1981, **103**, 6495.
16 S. Fukuzumi, Y. Kondo, and T. Tanaka, *Chem. Lett.*, 1983, 485.
17 A. Ohno, S. Yasui, R. A. Gase, S. Oka, and U. K. Pandit, *Bioorg. Chem.*, 1980, **9**, 199.
18 J. A. A. Ketelaar, C. V. Stope, and H. R. Gersmann, *Recl. Trav. Chim.*, 1952, **70**, 499.
19 A. Kitani and S. Sasaki, *Nippon Kagaku Kaishi*, 1978, 817.
20 A. Kitani, N. Hashimoto, and K. Sasaki, *Nippon Kagaku Kaishi*, 1978, 1103.
21 W. J. Blasel and R. G. Haas, *Anal. Chem.*, 1970, **42**, 918; F. M. Martens and J. W. Verhoeven, *J. Photochem.*, 1983, **22**, 99.
22 D. Mauzerall and F. M. Westheimer, *J. Am. Chem. Soc.*, 1955, **77**, 2261.
23 I. Fujita and H. Kobayashi, *Ber. Bunsenges. Phys. Chem.*, 1972, **70**, 115.
24 E. E. Wegner and A. W. Adamson, *J. Am. Chem. Soc.*, 1966, **88**, 394.

Received 12*th November* 1984; *Paper* 4/1951